# Protocol Proximity-1 Simulator for Telemetry on Mars Missions

Francisco Maia [a] *

Thesis to obtain the Master of Science Degrees in Electrical and Computer Engineering (IST) – January 2021

Supervisors: Prof. António Rodrigues [a, b], Prof. José Sanguino [a, b]

[a] *Instituto Superior Técnico (IST), Universidade de Lisbon, Portugal*
[b] *Instituto de Telecomunicações of Instituto Superior Técnico (IT)*
* *E-mail: francisco.maia@tecnico.ulisboa.pt*

---

**ABSTRACT**: "Mankind is drawn to the heavens for the same reason we were once drawn into unknown lands and across the open sea. We choose to explore space because doing so improves our lives, and lifts our spirit. So let us continue the journey"– George W. Bush. The race for space exploration has been increasing substantially, following the rapid technological development in recent years. In 2013, the Consultative Committee for Space Data Systems (CCSDS), formed by numerous space agencies - such as China National Space Administration (CNSA), Federal Space Agency (FSA), European Space Agency (ESA) and National Aerospace and Space Administration (NASA) – recommended a new standard protocol for space communications between spacecrafts in close proximity. This protocol is called Proximity-1 Space Protocol.

Proximity-1 describes recommendation standards for the two lowest layers of the Open Systems Interconnection (OSI) Model – Data Link Layer and Physical Layer. Both layer's recommendation will be taken into consideration in this simulator.

The purpose of this work is to simulate data transfer between two space vehicles (orbiter, lander or rover) according to the Proximity-1 Space Link Protocol and draw conclusions regarding its performance – percentage of error frames received, modulation and demodulation processes, data flow between sublayers, as well as its processing times, among others. Moreover, one could simulate any vehicle (orbiter, lander or rover) that needs to comply with the Proximity-1 standards.

The simulation allows analyzing in detail the proximity-1 protocol operations and interoperability between sublayers, contributing for a better understanding of each process. With this simulator, it is possible to adjust the protocol's different parameters - transmission power of each space vehicle, signal to noise ratio of the transmission channel, number of samples per bit, filters applied in the demodulation process, among others. Moreover, the simulation enables the flow of data, analyzing each step of the process, since the formation of a data packet, converting it into a modulated signal and vice-versa.

Regarding the Physical Layer, a Binary Phase Shift Keying (BPSK) modulator and demodulator are presented. The demodulator was tested in three different ways: using a *Costas Loop* algorithm, a *Phased Locked Loop* algorithm and an adaptation of the *Phased Locked Loop*. The main goal is to synchronize the frequency and phase of the receiving signal that suffers interference, and hence receive the transmitted data seamlessly.

Unlike the Physical Layer, the Data Link Layer is made up of separate blocks – sublayers – that cooperate to transform the received bitstream into data and vice-versa. Each block is asynchronous and has its own processing time that operates independently in a non-sequential order. Each sublayer has its own task: decode the received bits, group them into frames, monitor them, and give internal directives. These two layers are the backbone of protocol Proximity-1 Simulator.

**KEYWORDS**: BER, BPSK, Costas Loop, Data Link Layer, demodulator, frame, lander, modulator, Phase Locked Loop, Physical Layer, rover, orbiter, transceiver, white Gaussian noise.

---

## 1. INTRODUCTION

"This year has also been an inflection point in aerospace, with NASA committing to send astronauts to the moon once again, government programs all around the world taking huge strides towards a new era of globalized space exploration" (TIME, July 8, 2019). Therefore, research and development of radio communications should keep up the same pace, as they have an important role in space exploration. Short range communications (surface-to-orbit) are necessary for data transfer between vehicles (rovers and orbiters). In previous space missions, there was a direct communication link between the rover and Earth, which meant a rover should be capable of transmitting data back to Earth. Furthermore, a rover had limited resources regarding the transmission rate and power consumption leading to the fact that data could being sent relatively slowly with a weak signal. In response, a new protocol was created. Protocol Proximity-1 was developed to establish a communications protocol among orbiters, landers and rovers.

For instance, data is transmitted from a rover to a lander, both on Mars surface, then to a Mars orbiter, that, in turn, transmits the information back to an Earth orbiter or directly to an Earth station on its surface. Thereby, the rover does not require a heavy structure neither computation complexity to ensure the transmission of data directly to Earth. The information travels a shorter distance, from the rover to the lander and to the orbiting orbiter on Mars. This way, we mitigate the error rate and improve the bitrate, since an orbiter or a lander can have a more robust engineered structure to transmit data than a rover can. Proximity-1 Space Link protocol approved by the Consultative Committee for Space Data Systems (CCSDS) is an important benefit for orbiters, landers and rovers, therefore improving future Mars explorations.

## 2. PROXIMITY-1 PROTOCOL STANDARD – DATA LINK LAYER

The Proximity-1 protocol specifications can be found in CCSDS recommended standards [1], [2], [3] and [4]. "The Proximity-1 protocol is a bi-directional Space Link Protocol designed for the purpose of proximate communications among probes, landers, rovers, orbiting constellations, and orbiting relays" (*Source: [1]*). Data Link Layer and Physical Layer are two of the seven layers of the Open Systems Interconnection (OSI) model that are implemented in this protocol. Data Link Layer is divided into two parts, the sending side and the receiving side. *Figure 2.1* shows an overall overview of the connections between all sublayers both from the sending and receiving side.

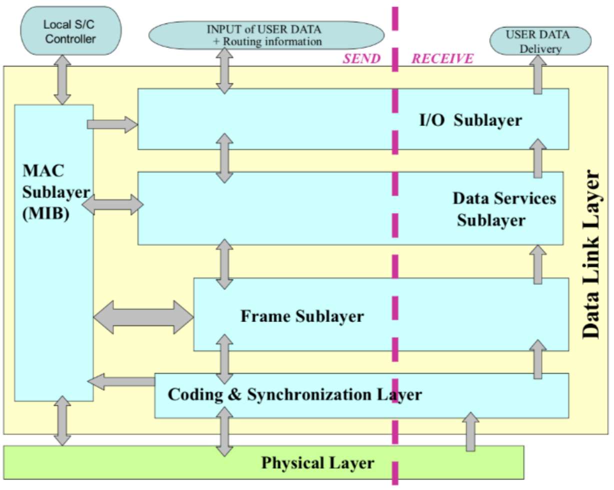


Figure 2. 1 Simplified diagram of Proximity-1 Layers (Source: [1]).

The sending side is responsible for the data processing since the input from the On Board Computer until sending a bitstream to the Physical Layer, while the receiving side receives a bitstream and converts it into data to be sent to the OBC. The Data Link Layer has 5 sublayers. The I/O Sublayer is responsible for the interface between the OBC and the Data Link Layer, by sending or receiving data packets from other sublayers, usually the Data Service Sublayer. This sublayer has the task to supervise the Communication Operation Procedure and to count the number of sent and received frames. Data Services Sublayer transmits its data to the Frame Sublayer that, in turn, selects a Version-3 Transfer Frame type. The selection procedure follows a priority list. The selected frame is then sent to the Coding and Synchronization Sublayer where an identifier called Attached Synchronization Marker (ASM) and a checksum (CRC) are attached to the transfer frame. The ASM, transfer frame and checksum form a data unit called Proximity Link Transmission Unit (PLTU). The PLTU will be sent as a bitstream to the Physical Layer to be converted into a modulated signal that can be transmitted through space by an antenna. The Medium Access Control Sublayer is connected to all sublayers and forwards directives.

According to the protocol, there are different types of data that are exchanged between sublayers. There are two types of Service Data Units, protocol-frames or user-frames. Protocol frames are used inside Proimity-1 protocol for configurations or directives, while user-frames contain data to be transmitted between transceivers. The I/O Sublayer receives Service Data Units and forms Version-3 Transfer Frames that has two separate fields: a transfer frame header and a transfer frame data field. The structure of a Version-3 Transfer Frame is shown in *Figure 2.2*.

The Transfer Frame is converted into a Proximity Link Transmission Unit inside the Coding and Synchronization Sublayer by attaching an Attached Synchronization Marker (ASM) in the beginning of the frame and a Cyclic Redundancy Check (CRC) at the end. In fact, the PLTU is the Data Unit base structure that is transmitted across space to the remote transceiver. *Figure 2.2* represents the structure of a PLTU. This transmission unit might be encoded by the Coding and Synchronization Sublayer prior to the transmission, if required.

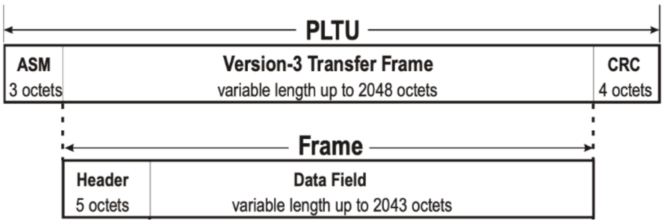


Figure 2. 2 – Proximity Link Transmission Unit structure (Source [2]).

In addition, the frame that is sent inside the PLTU has a Quality of Service assigned. This is an important parameter that impacts the COP procedure. There are two quality of services that a frame can have, the Expedited frame and the Sequence Controlled frame. The Sequence Controlled service is more reliable than the Expedited service, as a result of using a go-back-n Automated Repeat Queuing (ARQ) algorithm. Moreover, this algorithm guarantees a correct reception, meaning that it requires the receiver to emit a signal when a sequence controlled frame is received. This process is called the acknowledgement. On the other hand, Expedited services do not require any acknowledgement from the receiver. Nonetheless the quality of service has higher priority than a sequence controlled service.

## 3. PROXIMITY-1 PROTOCOL STANDARD – PHYSICAL LAYER

The Physical Layer is the lowest layer on the OSI Model. This protocol also takes this last layer into consideration which is the backbone for establishing a communication session. The Physical Layer's main purpose is to establish a communication channel between two transceivers by converting the serial bitstream, sent by the Coding and Synchronization Sublayer, into a modulated signal that, in turn, will be transmitted across space in a form of an electromagnetic wave as well as receiving the signal, demodulating it and converting it into a bitstream.

There are several parameters to configure the communication session, frequency, polarization, modulation, acquisition, idle sequence and the coded symbol rates.

A communication link is established upon a frequency channel, and it might require one or more frequency channels. The Ultra High Frequencies are between 300MHz and 3GHz, with the wave length ranging from one meter to one-tenth of a meter. The frequency range for the Ultra High Frequency (UHF) Proximity-1 links consists of 60 MHz between 390 MHz and 450 MHz with a 30 MHz guard-band between forward and return frequency bands. The forward frequency band shall be from 435 to 450 MHz, while the return frequency band shall be from 390 to 405 MHz. (*Source* [3]). The selection of the frequencies is subject to Space Frequency Coordination Group (SFCG) recommendations.

For interoperability at UHF, the default hailing channel shall be Channel 1 configured for 435.6 MHz in the forward link and 404.4 MHz in the return link. If the Proximity link radio equipment supports only a single channel (i.e., a single forward and return frequency pair), then the hailing channel shall be the same as the working channel. If the Proximity link radio equipment supports multiple channels, then the hailing channel shall be different from the working channel. After link establishment through hailing is accomplished, transition to the working channel (if available) should be done as soon as possible.

Forward and return link frequencies may be coherently related or non-coherent. The following three additional channels 1 to 3 (fixed single forward and return frequency pairs) are well defined for Proximity-1 operations, whereas for the following channel numbers there is a frequency range that is available.

The following *Table 3.1* details Proximity-1 channel assignments from 0 through 7.

Table 3. 1 - Proximity-1 channel assignments

| Channel Number | Forward Frequency [MHz] | Return Frequency [MHz] |
|---|---|---|
| 0 | 437.1 | 401.585625 |
| 1 | 435.6 | 404.4 |
| 2 | 439.2 | 397.5 |
| 3 | 444.6 | 393.9 |
| 4, 5, 6 and 7 | Within 435 to 450 | Within 390 to 405 |

Channels 8 through 15 are defined in the SET PL EXTENSIONS directive (see annex A). The assignment of specific frequencies to these channels is reserved by CCSDS.

In the case where there is a need for one or multiple return frequencies paired with one or multiple forward frequencies, the forward frequencies shall be selected from 435 to 450 MHz band in 20 kHz steps and the return frequencies shall be selected from 390 to 405MHz in 20kHz steps. These frequency pairs shall be distinct from the frequency pairs defined in Channels 0 through 7. The forward and return frequency components of Channels 8 through 15 are reserved for this purpose. (*Source* [3])

The Pulse Code Modulation (PCM) data is Bi-Phase-L encoded (also known as Manchester code) and it is directly modulated into the carrier. The residual carrier shall be provided with modulation index of 60º ±5%. The symmetry of PCM Bi-Phase-L waveforms shall be such that the mark-to-space ratio is between 0.98 and 1.02. For directly modulated Bi-Phase-L waveform, a symbol '1' shall result in an advance of the phase of the radio frequency carrier at the beginning of the symbol interval, while a symbol '0' shall result in a delay, as *Figure 3.1* represents. (*Source* [3])

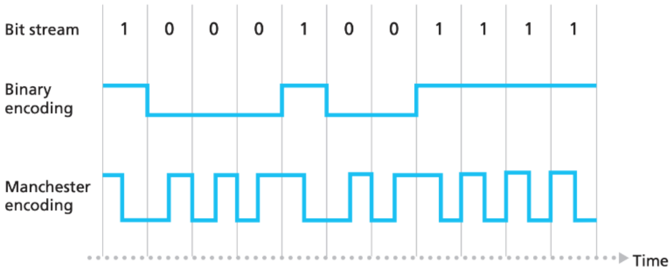


Figure 3. 1 - Bi-Phase-L encoding *(source: [28] Stanford Computer Science Department)*

Regarding the Polarization, this protocol operates with Right Hand Circular Polarization (RHCP) for both forward and return links.

## 4. MATLAB SIMULATOR

In order to have a better understanding of this complex protocol, a simulation of the Physical Layer and Data Link Layer was developed in MATLAB. This chapter describes the MATLAB simulator, detailing the two lowest layers of the OSI Model (Data Link and Physical Layers) according to the Proximity-1 protocol recommended standards. In addition, the following sections detail the interoperability between layers.

### Simulator Architecture Overview

The global structure of the simulator consists of two transceivers that transfer information between each other, transceiver A and transceiver B (they represent a rover, a lander or an orbiting orbiter). The simulator has two main blocks, the first block corresponds to the On Board Computer that loads data into buffers before entering the I/O Sublayer, and the second block corresponds to the Data Link Layer and Physical Layer processes.

The first block consist of a loading cycle that allows the On Board Computer to choose the Type of Protocol Data Unit (User Data-‘0’ or a Protocol Data-‘1’), also the Quality of Service (Expedited frames-‘0’ or Sequence Controlled frames-‘1’), and finally the data packet. These three components are inserted in the first position of a cell array (acting as a buffer). Additionally, this buffer is the input for the I/O Sublayer.

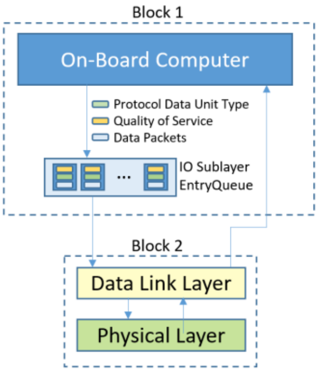


Figure 4. 1 – Simulator Architecture detailing Block 1.

The second block corresponds to the interoperability between the Data Link Layer and Physical Layer. Once the first cycle loads its data into a buffer called I/O Sublayer Entry Queue, the processing begins. Inside the Data Link Layer, each sublayer is interspersed by buffers, where information is written or removed. Since there are two transceivers, and each has its own variables, the same principle applies to the sending and receiving sides, since buffers have different purposes (either sending or receiving) and the values received must not be mixed up with the values to be transmitted.

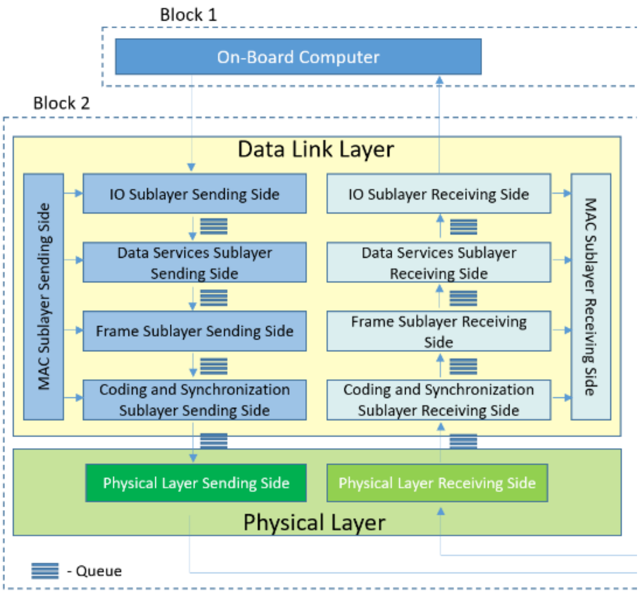


Figure 4. 2 – Simulator Architecture detailing Block 2.

The flow of data between transceivers depends on the quality of service of the frame sent. In case a frame has Expedited quality of service, the flow of data starts at transceiver A and arrives at transceiver B. However, if the frame has a Sequence Controlled quality of service, the flow of data starts at transceiver A, arrives at transceiver B, and requires an acknowledgement of the received frame. Therefore, the transceiver B transmits a PLCW frame – an acknowledgement - indicating the initial sender (transceiver A) that the frame was received. This acknowledgement also informs the sender whether the frame requires retransmission. *Figure 4.1* illustrates this procedure, known as the frame acceptance and reporting mechanism.

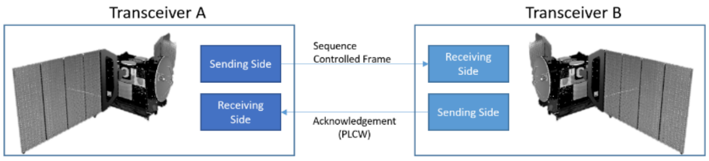


Figure 4. 1 – Frame acceptance and reporting mechanism.

For the second block, both Data Link Layer and Physical Layer must operate independently, meaning asynchronously. In MATLAB there is no function that allows multithreading. As such, the second cycle has a Tik system, similar to a master clock that serves as a reference to each sublayer. All Sublayers have different processing times due to their different tasks. This way, it is assigned a specific amount of Tiks (time unit) according to their complexity. This system allows each sublayer to work independently. In fact, this solution allows having a multithreading system that MATLAB does not grant.

The single unit of time called Tik corresponds to 0,2ms - the fastest processing time of a sublayer, from a 100-test experiment in real time.

Table 4. 1 - Sublayer’s Tik durations

| | **Transceiver A** | | **Transceiver B** | |
|---|---|---|---|---|
| | **Send Side** | **Receive Side** | **Send Side** | **Receive Side** |
| **IO Sublayer** | 3 | 4 | - | 4 |
| **Data Services Sublayer** | 2 | 3 | 1 | 3 |
| **Frame Sublayer** | 3 | 10 | 3 | 10 |
| **Coding and Synchronization Sublayer** | 10 | 1 | 10 | 1 |
| **Physical Layer** | 2000 | 1000 | 1650 | 1000 |

**Physical Layer Simulation**

The Physical Layer receives a bit stream provided by the Data Link Layer, more specifically, by the Coding and Synchronization Sublayer. This bit stream is converted into squared pulses, and then to polar data with Manchester Encoding, were the message is stored (*Figure 4.2*).

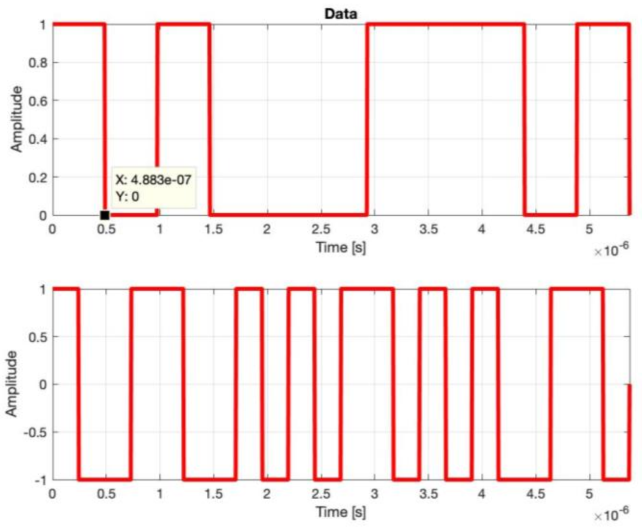


Figure 4. 2 – Converting binary data into a Manchester encoding message.

In the frequency domain, the Nyquist criterion states that the sampling frequency must be higher than twice the bandwidth in order to avoid aliasing ($f_s > 2B$). Whereas, in time domain the sampling rate (or sampling frequency) is the number of data samples acquired per second ($f_s = \frac{1}{\Delta t}$), where $\Delta t$ is the amount of time between data samples. The smaller the $\Delta t$, the better the chance of measuring the correct wave form. If it is considered a transmission data rate of 2,048 Mbps, each bit period corresponds to 48,8 µs. The simulations were performed with different values of samples per bit (detailed in sections 5.2 and 5.3). Moreover, each bit was represented by 3 carrier periods due to demodulation processes that are described in the receiving side. The modulated signal according to Proximity-1 protocol must be as follows:

$$mSig(t) = \sqrt{2P_t}\, sin(2\pi f_c t \; + \; \beta m(t) + \; \theta_c) \qquad (4.1)$$

The value β is the modulation index, that according to Proximity-1 protocol is $\frac{\pi}{3}$ (60º ±5%). $P_t$ is the transmitted power (in *Figure 4.2* $P_t$=1) and $\theta_c$ is the phase carrier. The *Equation 4.1* can be rewritten as follows:

$$mSig(t) = \sqrt{2P_t}\sin(2\pi f_c \mathrm{t} \; + \; \beta \mathrm{m(t)} + \; \theta_c) \qquad (4.1)$$
$$= \sqrt{2P_C}\sin(2\pi f_c \mathrm{t} \; + \; \theta_c) + \sqrt{2P_D} m(t)\cos(2\pi f_c t \; + \; \theta_c) \qquad (4.2)$$

From the *Equation 4.2* there are two signal components, a residual carrier ($\sqrt{2P_C}\sin(2\pi f_c \mathrm{t} \; + \; \theta_c)$) and a message carrier ($\sqrt{2P_D} m(t)\cos(2\pi f_c \mathrm{t} \; + \; \theta_c)$). This simplification is very useful for extracting the frequency and phase of the received signal. Another simplification considered from *Equation 4.1* to *4.2* is the following: $P_C = P_t\,(\cos\beta)^2$ and $P_D = P_t\,(\sin\beta)^2$.

From the receiving side, the demodulation process begins by filtering the received signal with a bandpass filter. The filter is centered at frequency $f_c$, which was obtained by applying a Fast Fourier Transform to the received signal and finding its maximum value. The error extracting the residual carrier is proportional to the width of the bandpass filter. The narrower the better, although, if the filter is too narrow, the magnitude of the signal might decrease significantly, due to the smooth cutoff frequency. 435.6 MHz is the recommended standard frequency for channel 1 as the hailing channel for forward link establishment, see page 3-16 of reference [1]. Due to filtering specifications, the magnitude of the signal decreases after filtering with a 4th order Butterworth lowpass filter.

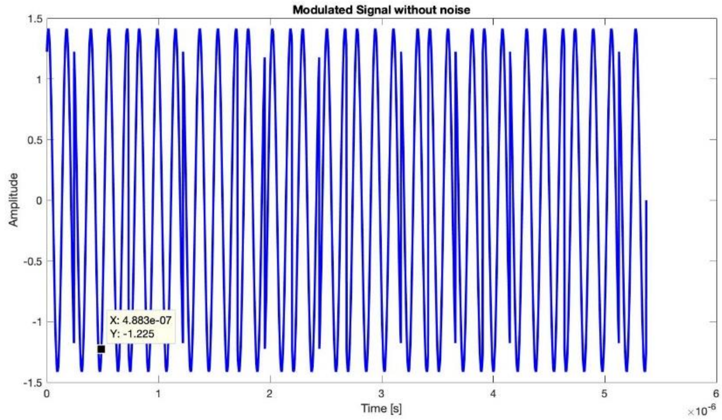


Figure 4. 3 - Modulated signal mSig(t)

Once the frequency is obtained, the next step is finding the phase. Thus, a comparison is made between a signal with phase zero and the received signal, both with the same frequency. Hence, the frequency and phase of the received signal are now known. Therefore, an artificial cosine is generated with the same frequency and phase as the residual carrier, and it is multiplied with the received signal. The product is then allocated into the input of a Low Pass filter, where the output is the message demodulated. In order to recover the data from the recently demodulated signal, a technique called integrate and dumping is used. *Figure 4.3* represents a demodulated signal, it is not a perfect squared signal due to Bandpass and Lowpass filters characteristics. Comparing to *Figure 4.2*, the demodulated signal is very similar to the original message.

$$Received\ Signal = \sqrt{2P_t\,(\cos\beta)^2}\sin(2\pi f_c \mathrm{t} \; + \; \theta_c)$$
$$+ \sqrt{2P_t\,(\sin\beta)^2} m(t)\cos(2\pi f_c t \; + \; \theta_c) \qquad (4.4)$$

$$Residual\ Carrier = \sqrt{2P_C}\sin(2\pi f_c \mathrm{t} \; + \; \theta_c) \qquad (4.6)$$

The artificial sine wave must be a cosine, otherwise the message would be eliminated after the Low Pass Filter. The following Equations demonstrate how the message is demodulated.

$$\Big[\sqrt{2P_t\,(\cos\beta)^2}\sin(2\pi f_c \mathrm{t} \; + \; \theta_c)$$
$$+ \sqrt{2P_t\,(\sin\beta)^2} m(t)\cos(2\pi f_c t \; + \; \theta_c)\Big]$$
$$\times\; \mathrm{A_0}\cos(2\pi f_c t \; + \; \theta_c) \qquad (4.7)$$

After the Low Pass Filter the signal is the following:

$$\frac{A_0\sqrt{2P_t\,(\sin\beta)^2}m(t)}{2} \tag{4.8}$$

*Equation 4.8* is represented on *Figure 4.3*, considering $A_0 = 1$, $P_t = 1$ and $\beta = \frac{\pi}{3}$, which results in $0.6m(t)$, approximately. Depending on the amplitude of the artificial cosine - $A_0$ - and the transmission power - $P_t$ - the message might be closer to the original sent message.

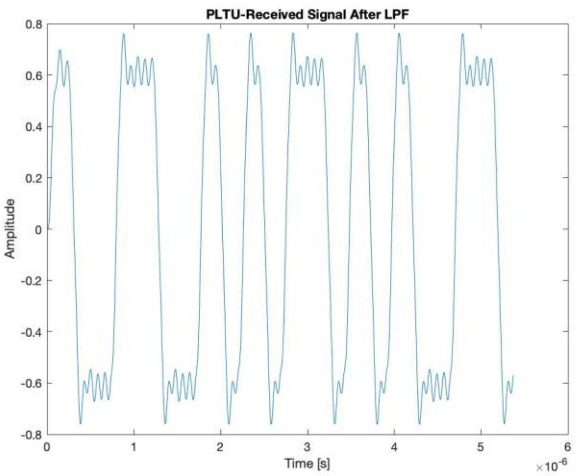


Figure 4. 4 – Demodulated signal

*Figure 4.5* represents the simplified block diagram used to demodulate the received signal.

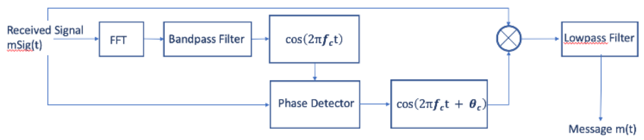


Figure 4. 5 – Block diagram used to demodulate the Received Signal

### Data Link Layer Simulation

The Data Link Layer processes all the data across all sublayers between the On-Board Computer and the Physical Layer. Considering that each sublayer has a sending side and a receiving side, there is a separate function for each side. Although they are different functions, a sublayer is the combination of both sending and receiving sides. All the processes implemented comply with the proximity-1 protocol's recommended standards, detailed in section 2.

## 5. RESULTS & DISCUSSIONS

This chapter covers several details of the implementation in MATLAB, which had to be considered to make the protocol compatible within its functions and capabilities — particularly data processing variables, how to improve the Communications Operations Procedures.

Furthermore, *Chapter 5* considers different communication scenarios. It discusses ways of simulating different transceivers (orbiter, lander or rover) and the different environments between them, considering noise, atmosphere, fading, among others. Thus, the signal-to-noise ratio will vary, as will the power of the signal emitted. Likewise, the type and order of the filters are changed, to analyze its effect on the received demodulated signal.

Finally, this section describes operational issues and presents future recommendations.

### 5.1. Processing Times

In this simulation, each unit of time, designated as a Tik, is approximately 0,2 milliseconds. This time was obtained experimentally using the MATLAB tik-tok integrated function. The time was measured once the sublayer function was called until the end of its processing. Every simulation was carried out in a similar test environment, that is, with the same conditions from the beginning until its completion.

The computer processor was used both for running the simulation in MATLAB and for other system tasks. Between each simulation the usage of the processor was minimized, in order not to interfere with the performance of the simulation. Therefore, of the one hundred experiments carried out, the time considered and allocated to each sublayer corresponds to the shortest time recorded and not the average of the collected times.

The main reason for this decision lies on the fact that, if each sublayer was able to execute the task in that reduced time, it means that in an ideal environment (where the protocol implementation has a dedicated processor) it would also execute it in that short amount of time.

The processor used in this experiment has an iOS operating system with 16GB ram memory processing capabilities, 2.7 GHz Intel Core i5 dual core. In order, not to limit the processing time conditioned by the processor (technology is constantly evolving), one considered the Tiks as relative time units between sublayers, thus reflecting a comparative time period between processor-independent functions.

Evidently, every sublayer will have its processing time depending on the degree of complexity of its operations. Moreover, it would be expected that the functions that represent sublayers on transceiver A would have similar processing times as those on transceiver B – in case transceivers are the same vehicle. Ideally, they would have the same processing time. However, in table 4.1 we considered two scenarios for Transceiver A and B. Transceiver A transmits every type of frame, while transceiver B transmits only PLCW frames – acknowledgements. On the transmission side, it was not considered in the simulation the I/O Sublayer to be able to choose the type of frame inserted, since it is programmed to send protocol frames (PLCW – acknowledgements) and not to receive information from the On-Board Computer. Therefore, the processing time of this sublayer was omitted.

### 5.2. Acknowledgement Ensurance

During the FARM process, during the transmission of the acknowledgement, an error may occur in the reception.

Therefore, measures will have to be taken to prevent this situation. For example, if transceiver A does not receive a PLCW in the expected time, transceiver B will have to retransmit the PLCW frame. In addition, in case the PLCW comes with errors, transceiver B will also have to retransmit. The retransmission of a PLCW is not included in the protocol and is good addition to future protocol developments.

### 5.3. Signal Demodulation

In a signal demodulation process, an important factor to be considered is the filter's type choice. There are many filters that can be used to demodulate a signal. Due to computational efficiency, the higher order filters require more time to filter the signal. The higher the order of the filter, the longer it will take for the filter to process the final resulting signal. Thus, it must be a compromise between a sharper cut-off frequency and the time to process filtering the signal. In this dissertation, the ones used are the Band Pass Butterworth filter followed by a Low Pass Butterworth filter. The Band Pass Butterworth filter is applied with 1st order, and a band pass of 20 MHz. While the second filter is a Low Pass 4th order Butterworth filter.

In conclusion, the filter used in this MATLAB simulation is the Butterworth filter due to its smooth pass-band and stop-band characteristics, with a 4th order for a sharp cut-off frequency. A higher order will have a sharper cut-off, but the processing time will be higher, compromising the efficiency.

### 5.4. Discussion - Different Scenarios

This dissertation aims to simulate and analyze the data transmission between three space vehicles —orbiter, lander and rover. In order to bring this simulator closer to reality, it is necessary to take into account several factors such as the planet's atmosphere, fading, free space path loss and line of sight, as well as the different transmission powers associated with each of these vehicles.

In the transmission channel, there are three main factors that affect the signal, these are: Free Space Path Loss (FSPL), Fading and Line of Sight.

#### Free Space Path Loss

Free space path loss occurs to the electromagnetic waves, when propagating in the atmosphere, suffering an opposition directly proportional to the distance it travels. Considering isotropical antennas ($G_s = G_r = 0\ dB$), the free space path loss ($A_0$), represented in *Equation 5.3*, is based on *Friis* equation represented in *Equation 5.3*.

$$\lambda = \frac{c}{f_{[Hz]}}\ ;\ \ c = 3 \times 10^8\ \text{m/s} \tag{5.1}$$

$$\frac{P_r}{P_t} = G_r G_t \left(\frac{\lambda}{4\pi d_{[m]}}\right)^2 \tag{5.2}$$

$$A_0 = -10 \log\left(\frac{\lambda}{4\pi d_{[m]}}\right)^2\ \ [\text{dB}] \tag{5.3}$$

From *Equation 5.3*, it is possible to calculate the free space path loss. The frequency may vary from 435,6 MHz to 450,0 MHz on the send side, while the return frequency varies from 390 MHz to 405 MHz. These frequency amplitudes do not interfere significantly to the signal attenuation. However, the distance between transceivers is an important factor that affects the transmitted signal. There are three different scenarios for each communication session, represented in *Table 5.1*.

In addition, it must be taken into consideration the line of sight between the orbiter and lander, since the orbiter is not in a geostationary orbit. This is represented in *Figure 5.1*. The maximum distance capable of establishing a communication session link is $d_{max}$.

$$d_{max} = d_{rh1} + d_{rh2} \tag{5.4}$$

$$(R + h_1)^2 = R^2 + {d_{rh1}}^2 \tag{5.5}$$

$$d_{rh1} = \sqrt{2Rh_1} \quad (R \gg h_1) \tag{5.6}$$

$$(R + h_{orb})^2 = R^2 + {d_{rh2}}^2 \tag{5.7}$$

$$d_{rh2} = \sqrt{2Rh_{orb}} \quad (R \gg h_{orb}) \tag{5.8}$$

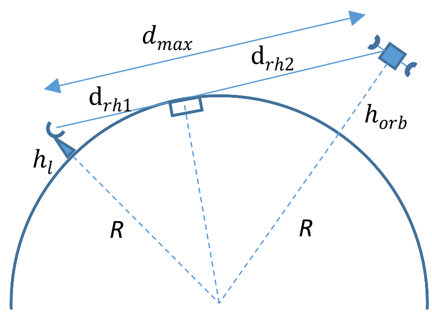

Figure 5. 1 – Line of sight between a lander and an orbiter.

Considering that Mars radius is 3389,5 km, the height of the lander is 5 m, and the height of the orbiter from Mars surface is 255 km, the maximum distance is 1320,6 km. Thus, the FSPL, in this scenario, is 146,7 dB (for a frequency channel of 390 MHz) and 147,9 dB (for a frequency channel of 450 MHz).

The last scenario considered in *Table 5.1* corresponds to a communication link established between a lander and a rover on Mars surface. In this case, similarly to the previous scenario and due to Mars round surface, it also must be taken into account the line of sight between both transceivers. There is a maximum distance where the lander can no longer maintain a communication session with the rover, since it is not on lander's sight anymore. Considering $h_{orb} = h_1$, *Figure 5.1* also illustrates how far the horizon is from the lander's antenna (radio-horizon distance - $d_{rh}$), as well as the maximum distance between the rover's and lander's antennas in order to keep a line of sight among both transceivers - assuming the antennas are at the same height.

*Equations 5.9* and *5.10* represent the line of sight formula, where *R* represents Mars radius, and *h* the height of the antenna. Moreover, this formula assumes there are no relevant obstacles interfering with the signal between the antennas.

$$(R+h)^2 = R^2 + {d_{rh}}^2 \quad (5.9)$$

$$d_{rh} = \sqrt{2Rh} \quad (R \gg h) \quad (5.10)$$

Considering Mars radius to be 3389,5 km, the radio-horizon distance ($d_{rh}$) is 5.8 km. If the Rover's antenna has the same height as the Lander's, the maximum horizon distance is twice the $d_{rh}$ (11.6 km). Therefore, the FSPL for the third scenario is 106 dB. For more detail please see reference [15].

Table 5. 1 – Free space path loss for different scenarios.

| **Scenarios** | $L_{fs}$ for **Forward Channel Frequency (450MHz)** | $L_{fs}$ for **Return Channel Frequency (390MHz)** |
|---|---|---|
| **Earth orbiter - Mars orbiter ($400 \times 10^6$ km)** | 257,5 dB | 256,3 dB |
| **Earth orbiter - Mars orbiter ($54,6 \times 10^6$ km)** | 240 dB | 239 dB |
| **Mars orbiter – Lander/Rover (1320,6 km)** | 147,9 dB | 146,7 dB |
| **Mars orbiter – Lander/Rover (255 km)** | 133,6 dB | 132,4 dB |
| **Lander – Rover (11,6 km)** | 106,8 dB | 105,6 dB |

As expected, the Free Space Path Loss increases with the distance between transceivers.

**Fresnel Ellipsoid and Elevation Angle**

Considering the scenario of a communication link established between a lander and an orbiter as illustrated on *Figure 5.1* and *Figure 5.2*, it is a reasonable approximation to neglect the height of the lander compared with the height of the orbiter. Therefore, when the orbiter is the farthest apart from the lander, but still in line of sight, it is common to consider an elevation angle of 0º. In addition, in order to avoid nearby interferences by the surrounding terrain roughness, it is enough to have an elevation angle of 5º. If the angle of the lander's antenna is negative, the signal will not reach the orbiter with the desired strength. If the angle of transmission is 5º, the less likely it is to have objects interfering with the Fresnel ellipsoid. In contrast, if the transmission angle is *null*, half the Fresnel ellipsoid is blocked by Mars' surface and hence the signal power is reduced by half its value. To calculate the radius of Fresnel ellipsoid between the antennas, *Equation 5.11* is used, where n is the obstacle number at distance $d_k$, while $d$ is the total distance between antennas and $\lambda$ is the wavelength ( $\frac{c}{f}$ ).

$$r_{[m]} = \sqrt{\frac{n \times \lambda \times d_k(d-d_k)}{d}} \quad (5.11)$$

For the distance ($d_k$) closer to the lander, the ellipsoid radius is not intersected by Mars surface, considering the antenna is not obstructed by considerable obstacle.

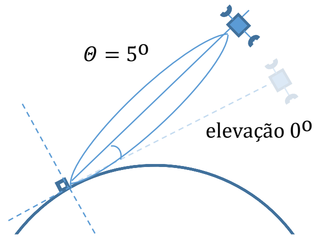


Figure 5.2 - Representations of Fresnel ellipsoid and transmission angle.

Accounting for the transmission angle of 5 degrees and the landers antenna having 5m height, the Fresnel ellipsoid does not contribute for the signal attenuation in this scenario – similar to an open plain - where the terrain allows it.

**Fading and Mars Atmosphere**

Another external factor to be taken into consideration is fading. This phenomenon is the fluctuation of the signal's amplitude between the sender and the receiver, caused by variations in the medium where electromagnetic waves propagate. There are two types of fading: power fading, corresponding to slow variations in the received signal, associated with atmospheric disturbances; and multipath fading, corresponding to fast variations in the received signal, due to the signal reaching the receiver from different paths.

Mars surface has rocks and hilly structures, reported by previous Mars missions (Pathfinder and Viking), that cause reflections on the radio waves, resulting in multipath fading phenomenon. Extrapolating from Earth-based experiments on similar rocky surfaces, the attenuation ranges from 2 to 7 dB for 870 MHz wave frequencies. So, for a lower frequency (400 MHz) it is expected to have a lower attenuation.

According to NASA (reference [16]), Earth and Mars have an atmosphere and ionosphere where radio waves suffer attenuations while propagating through them. At Mars the major attenuation factor is dust storms, which affect mostly frequencies around 32 GHz, with an attenuation of 3 dB (not relevant for the frequencies used in Proximity-1 protocol, around 400 MHz as described in previous subsections). Moreover, this type of storm is rare. Under normal conditions, a storm only attenuates the signal 1 dB. Additionally, there are no rain observation reports on Mars. In case there is rain in the planet, it would be so light that it would not cause significant attenuation to radio waves. The tropospheric losses - gaseous attenuation, cloud, fog, tropospheric scattering – scintillation and turbulence - account only 0.4 dB losses for frequencies around 32 GHz, which causes no considerable attenuation for frequencies around 400 MHz. Regarding the Martian ionosphere, there is also some absorption and scintillation effects on very high frequencies (VHF) - 100 MHz to 500 MHz

- around 0.5 dB. Comparing to Earth, the Martian ionosphere is one order of magnitude thinner.

*Table 5.2* sums up the major contributions for Mars radio wave attenuations. Usually, during space communications, there is a margin of 2% where the signal is interrupted. Half of these 2% corresponds to damaged material and atmospheric conditions; the other 1% is due to other causes. (reference [18]). Other attenuations might occur when a communication session is established between an orbiter and an Earth-based space station. In this case, the signal suffers an attenuation in the ionosphere. In this simulation, these scenarios were not considered, however to see in detail, please see reference [19]. .[1]

Table 5. 2 – Martian radio wave attenuation for very high frequencies.

| | **VHF (100 MHz – 500 MHz)** |
|---|---|
| **Ionosphere (absorption and scintillation)** | 0.5 dB |
| **Troposphere (scattering)** | 0 |
| **Gaseous** | 0 |
| **Cloud, Rain and Fog** | 0 |
| **Aerosol (haze)** | 0 |
| **Dust (worst case)** | 0.1 dB |
| **Total Vertical Losses** | 0.6 dB |
| **Multipath (for 870 MHz)** | 2-7 dB |

**Signal to Noise Ratio**

The signal to noise ratio (SNR) is an important factor to simulate the transmission channel.
The SNR may be calculated using the following Equation:

$$\mathrm{SNR} = \frac{P_{signal}}{P_{noise}} \quad ; \quad 10^{\frac{dB}{10}} = \frac{P_{signal}}{P_{noise}} \qquad (5.12)$$

The following *Figure 5.3* represents the percentage of error frames received by transceiver B while varying the signal to noise ratio. It is the result of approximately 6000 transmission-frame simulations (more than one hundred for each dot).

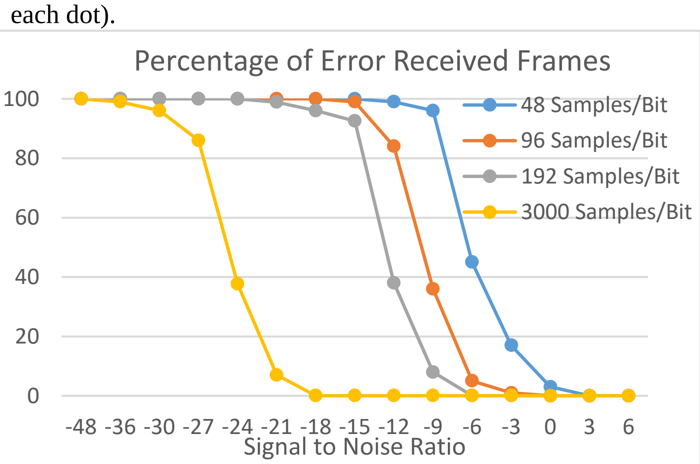

Figure 5. 3– Percentage of error received frames (Pt = 1 W).

[1] Note: in this simulation, the medium loss through interplanetary space is ignored.

As expected, for the same number of samples per bit, the increase of the signal to noise ratio, leads to fewer error frames received. Moreover, as the number of samples per bit increases, the fewer error frames received for the same SNR. In addition, the three curves representing different samples per bit are shifted 3dB from one another due to doubling the number of samples per bit.

On the following Equations, $L_{fs}$ stands for the free space path loss attenuation, while $L_a$ represents the atmosphere attenuation plus fading losses.

$$P_r[\mathrm{dBW}] = P_t[dBW] + G_r[dBi] + G_t[dBi] - L_{fs}[\mathrm{dB}] - L_a[\mathrm{dB}] \qquad (5.13)$$

$$L_{fs}[\mathrm{dB}] = 10log_{10}\left(\frac{\lambda}{4\pi d}\right)^2 \qquad (5.14)$$

$$P_r[\mathrm{dBW}] = 10\ \log_{10}(P_{[W]}/1[W]) \qquad (5.15)$$

Considering *Tables 5.1* and *5.2*, it is possible to estimate what is the received power by the receiving antenna for the different scenarios.

Furthermore, it is considered an antenna gain of 0 dBi for the receiver and a gain of 0 dBi for the transmitter.
It is considered a 5 dB attenuation for fading plus atmosphere attenuation. According to *Equation 5.13*, the received power is represented in *Table 5.3*.

Table 5. 3 – Antennas transmitting and receiving powers for different scenarios.

| **Scenarios** | $P_r[dBW]$ | $P_r[W]$ |
|---|---|---|
| **Earth orbiter - Mars orbiter (400 × 10⁶ km)** | -240,74 | $\mathbf{8 \times 10^{-25}}$ |
| **Earth orbiter - Mars orbiter (54, 6 × 10⁶ km)** | -223,24 | $\mathbf{4,74 \times 10^{-23}}$ |
| **Mars orbiter – Lander/Rover (1320,6 km)** | -131,14 | $\mathbf{7,69 \times 10^{-14}}$ |
| **Mars orbiter – Lander/Rover (255 km)** | -116,84 | $\mathbf{2,07 \times 10^{-12}}$ |
| **Lander – Rover (11,6 km)** | -90,04 | $\mathbf{9,9 \times 10^{-10}}$ |

Despite $\boldsymbol{P_r}$ values being very low, they are expected, since a communication session between space transceivers has a huge attenuation loss.

**Sampling Rate**

Since the beginning of this dissertation, it is considered that 1 bit requires three wave periods to be represented, and each wave period is represented by 100 sample units. Therefore, 1 bit has 300 sample units, which requires a high performance, complex and robust software and hardware to support the transmission for this amount of information, considering that a PLTU can go up to 2056 bytes (16448 bits). To remove this demanding scenario, one must lower the number of samples per bit, as illustrated in *Figure 5.3*.

### 5.5. Operational Issues

In this section, an enumeration is made of some operation issues that arose during the MATLAB implementation. The fact that a Sequence Controlled frame requires an acknowledgement (PLCW) validation to be able to send the message to the remote transceiver causes a delay in the communication channel. In a way, it causes a congestion in the waiting queue between sublayers. Thus, as a waiting queue has limited storage, it might reach a point where there is no storage left to allocate the Sequence Controlled frame and it has to be discarded. This is not only an operational problem but also harms the efficiency of data throughput transmission.

There are other parameters that spoil the data transmission efficiency, such as the retransmission of a Sequence Controlled frame, asymmetric data rates between transceivers, the frame lengths and the maximum transmission window size.

### 5.6. Future Developments and Recommendations

This protocol is called a single master topology, because the frame header can only address the source or the destination node, but not both. One future development might be to include the source and destination addresses in order to allow operating in a multicast topology.

For future developments, proximity-1 might include different scenarios for one-to-one topologies. There is the case where there are multiple one-to-one links, and each operates independently because each link has its own dedicated frequency channel pair. However, it might be useful to have a more dynamic environment, where there are separate hailing and working channels. Sharing a common hailing channel allows any spacecraft to contact any other spacecraft in that enterprise that uses the Protocol Proximity-1 recommended standards. Switching to a separate working channel is necessary because this releases the shared hailing channel to be used by either spacecraft. This “carrier sensing mechanism” is a good improvement for the Proximity-1 protocol.

## 6. CONCLUSION

The investigation and application of Protocol Proximity-1 proved to be able to establish a reliable communication session between two transceivers during a final approach to Mars.

Regarding the Physical Layer, the best way to demodulate the signal was not through the Costas Loop Algorithm, nor the Phase Locked Loop, but by applying a simpler and more effective demodulation process, detailed in *Chapter 4*.

Data Link Layer operates as expected, following the Protocol Proximity-1 recommended standards. Each sublayer operates independently, with different processing times, although there is interoperability between sublayers (the output data of a Sublayer is the input of another). The Processing times of each Sublayer vary greatly. The Physical Layer takes at least one hundred times longer than the Data Link Sublayers to conclude its processing, due to its more complex operations.

For the different scenarios of a communication link (between an orbiter, lander and rover) there are different attenuation factors affecting the transmission channel. From all the attenuation factors, the biggest contributor is the Free Space Path Loss due to the distance separating the two transceivers. Other factors that contribute to the attenuation of the transmitting signal are fading, Martian atmosphere, line of sight, Fresnel ellipsoid and the elevation angle. The medium loss through interplanetary space is ignored.

Regarding the demodulation, the preferable filter used is a fourth order Butterworth filter, due to the stopband and passband smoothness. The chosen fourth order was a compromise between sharpness and computational performance. The higher the order, the sharper the cut-off frequency. However, it takes a longer processing time to apply a higher order filter.

One improvement the Protocol should consider having in future developments is a frame header variable to identify not only the destination spacecraft ID, but a frame header section to identify the spacecraft ID source. This way, it allows operating in a multicast topology, addressing both source and destination nodes.

Regarding the acknowledgement process, there might be space to some improvements. The retransmission of PLCWs is an effortless improvement with a positive impact on the Protocol results. A solution might be adding a variable to block the transmission of Sequence Controlled frames until a valid PLCW is received, or establishing an expectable PLCW receiving time, that if a PLCW frame is not received in that period of time, a PLCW must be retransmitted, before sending another Sequence Controlled frame. This enhances the FARM process.

To sum up, this dissertation provides a scientific, technical and operational overview of the Protocol Proximity-1, promoting future developments in space explorations. In addition, provides and makes it possible for smaller satellites to have a say in space communications. This dissertation confirmed the protocol standard recommendations proved to be suitable for space explorations for short relay communications. Overall, this study pushes humanity a step further to mars and space explorations, as well as, it represents a big step in my personal career. Rephrasing Neil Armstrong’s famous quote in 1969, that is one small step for mankind, one giant leap for a man.

## REFERENCES


[1] CCSDS, Proximity-1 Space Link Protocol – Rationale, Architecture and Scenarios, Dec 2013, Informational report, CCSDS 210.0-G-2, Green Book, Washington DC, USA.

[2] CCSDS, Proximity-1 Space Link Protocol – Data Link Layer, Jul 2020, Informational report, CCSDS 211.0-B-5, Blue Book, Washington DC, USA.

[3] CCSDS, Proximity-1 Space Link Protocol – Physical Layer, Dec 2013, Informational report, CCSDS 211.1-B-4, Blue Book, Washington DC, USA.

[4] CCSDS, Proximity-1 Space Link Protocol – Coding and Synchronization Sublayer, October 2019, Informational report, CCSDS 211.2-B-2, Blue Book, Washington DC, USA.

[5] Eliasson, Malin and Hassel, Johan 2015. Architecture and Performance Evaluation of the Space Communication Protocol Proximity-1. Master of Science Thesis in Embedded Eletronic System Design. Chalmers University of Technology, University of Gothenburg, Sweden.

[6] Tofigh, Ehsan. 2016. Design and Implementation of High Performance BPSK Demodulator for Orbiter Communications. Master of Science Thesis in Aerospace Engineering. Delft University of Technology, Delft, Netherlands.

[7] Matias, André. 2014. Módulo de Comunicações Digitais para o ISTnanosat. Instituto Superior Técnico, Universidade de Lisboa, Lisboa, Portugal.

[8] TM Synchronization and Channel Coding. Issue2. Recommendation for Space Data System Standards (Blue Book), CCSDS 131.0-B-2. Washington, D.C.:CCSDS, August 2011.

[9] G.A. Leonov. 2006. Phase Synchronization: Theory and Applications. St. Petersburg State University, Russia.

[10] Barat, Aakriti. 2017. Analysis and Design of Phase Locked Loops with insight into Wavelet Analysis. Ohio State University, United States of America.

[11] K.Borre.2007. A software-Defined GPS and Galileo Receiver: A single-Frequency Approach. Applied and Numerical Harmonic Analysis. Birkhuser, Basel.

[12] M. K. Simon and S. Million. 1996. Residual Versus Suppressed-Carrier Coherent Communications.

[13] Manique, Inês. 2015. Cálculo da Atenuação numa Ligação Rádio Via-Ionosfera. Instituto Superior Técnico, Lisboa, Portugal.

[14] Mars Reconnaissance Orbiter, National Aeronautics and Space Administration [Online]. Available: https://mars.nasa.gov/files/mro/MRO-060303.pdf. [Accessed July 2020].

[15] Haslett, Christopher. 2008. Essentials of radio wave propagation, pp 118–120. Cambridge University Press.

[16] Propagation Issues for Communication between Earth and Mars, NASA Jet Propulsion Laboratory, Deep Space Communications and Navigation Center of Excellence [Online]. Available: https://descanso.jpl.nasa.gov/propagation/mars/MarsPub_sec7.pdf. [Accessed August 2020]]

[17] Microrover Radios and Antennas, NASA Mars Exploration Program, Mars Pathfinder [Online]. Available:https://mars.nasa.gov/MPF/rovercom/itworks.html.

[18] Maral, Gérard and Bousquet, Michel. 2009. Satellite Communications Systems, Systems, Techniques and Technologies. Wiley 5th edition. Toulouse, France.

[19] Capela, Carlos. 2012. "Protocol of Communications for VORSAT Satellite". Faculdade de Engenharia da Universidade do Porto, Portugal. Available: https://paginas.fe.up.pt/~ee97054/Transmission%20Losses.pdf.

[20] Recommendation ITU Radiocommunication Assembly, ITU-R SF.358-5. [Online] Available: https://www.itu.int/dms_pubrec/itu-r/rec/sf/R-REC-SF.358-5-199510-W!!PDF-E.pdf.

[21] Satellite Communications, Delta University. Egypt. [Online] Available: https://deltauniv.edu.eg/new/engineering/wp-content/uploads/Sat52015.pdf

[22] Ludwig, Roger and Taylor, Jim. March 2002. "Voyager Telecommunications - Design and Performance Summary Series Article 4". NASA Jet Propulsion Laboratory, Deep Space Communications and Navigation Center of Excellence [Online]. Available: https://descanso.jpl.nasa.gov/DPSummary/Descanso4--Voyager_new.pdf.

[23] Salema, Carlos. Feixes Hertzianos. 2002. IST Press.

[24] Balanis, Constantine A. Antenna Theory: Analysis and Design, 4th Edition. 2016 John Wiley.

[25] Hall, Barclay. Propagation of Radiowaves. Hewitt 1988 IEE Press.

[26] A 48/56/64 kbit/s Data Circuit-Terminating Equipment Standardized for Use on Digital Point-to-Point Leased Circuits. ITU-T Recommendation V.38. Geneva: ITU, 1996.

[27] Performance Characteristics for Intermediate Data Rate Digital Carriers Using Convolutional Encoding/Viterbi Encoding. Rev. 10. IESS 308. Washington, DC: INTELSAT, 2000.

[28] Stanford Computer Science Department. [Online] Available: https://www.scs.stanford.edu/09au-cs144/notes/l11.pdf

[29] Signal Processing. StackExchange. IIR filters. [Online] Available: https://dsp.stackexchange.com/questions/9745/which-iir-filters-approximate-a-gaussian-filter.

[30] CCSDS, Unified Space Data Link Protocol, Oct 2018, Recommended Standard CCSDS 732.1-B-1, Blue Book, Washington DC, USA.